Digital Twin Enabled Multi-Step Strategies for Autonomous Power Equalization in Optical Networks

CHENYU SUN[1,2,3,*], XIN YANG[1,4], GABRIEL CHARLET[1], PHOTIOS A. STAVROU[2], AND YVAN POINTURIER[1]

[1] Optical Communication Technology Lab, Paris Research Center, Huawei Technologies France SASU, Boulogne-Billancourt, France
[2] Communication Systems Department, EURECOM, Sophia Antipolis, France
[3] Sorbonne University, Paris, France
[4] Politecnico di Milano, Milan, Italy
[*] chenyu.sun1@huawei.com

Compiled March 5, 2025

This paper proposes and experimentally evaluates digital twin techniques incorporating multi-step lookahead and dynamic step-size adjustments for per-channel power equalization in optical networks. Digital twins, which are software replicas of physical systems, are utilized to monitor, analyze, and predict network behavior, thereby enhancing decision-making processes before implementing any physical adjustments. The study focuses on optimizing the signal-to-noise ratio (SNR) through per-channel launch power equalization, addressing challenges such as nonlinear inter-channel interference and power transfers across multiple optical multiplex sections. The proposed methodology leverages a digital twin to simulate and predict SNR variations using multi-step lookahead, ensuring monotonous SNR improvement without service disruptions. Additionally, parallel adjustment and dynamic step-size methods significantly enhance efficiency. Experimental validation on a C-band meshed optical network testbed demonstrates substantial reductions in power errors, improved SNR performance, and decreased commissioning time, highlighting the practical feasibility and efficiency of the approach. The findings underscore the transformative potential of digital twins in advancing autonomous optical network management.

http://dx.doi.org/10.1364/ao.XX.XXXXXX

1. INTRODUCTION

Digital twins (DT), are software replica of real physical systems, which can directly interact with the underlying physical system, have been proposed and used in optical networks for automation and management [1–4]. By monitoring its twin physical system, a digital twin can analyze the behavior of the underlying physical system using physical or machine learning models (or a combination of the two [5]). Then, the digital twin can be used as a sandbox to predict the impact of changes to the system through emulation within the digital twin, thereby improving decisions before implementing any operation in the physical world. A typical workflow using a digital twin is shown in Fig. 1.

Methods to optimize optical networks through per-channel launch power setting (also known as power equalization) based on physical models [6, 7] or machine learning models [8, 9] have been proposed and widely applied. Signal-to-noise ratio (SNR), as a significant criterion to assess the quality of transmission (QoT) of a communication system, can be improved thanks to power equalization. However, when networks are operating for a long time, e.g., in "set and forget" mode or after unforeseen events that change the underlying physical layer (e.g., span loss increase after repairing a fiber cut), power settings hence SNR

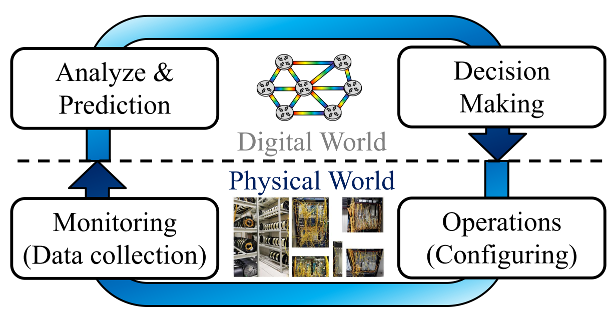

Fig. 1. Digital twin enabled closed-loop control.

may become suboptimal [10]. For this reason, it is important to periodically re-optimize the network.

Power equalization practically consists of adjusting the power of one or several channels of one or more optical multiplex sections (OMSs) through wavelength selective switch (WSS) per-channel attenuation change. Changing several channels' power on a single WSS is possible; however, simultaneously changing the settings of WSS on several OMSs, or even on the same OMS, is virtually impossible, such that WSS attenuation profile change can only be considered as sequential rather than parallel operations, and the impact of the change of one WSS attenuation profile, on OMSs downstream of said WSS, always needs to be considered when optimizing powers.

Specifically, when optimizing the power of a multi-OMS service, it is possible that the SNR of this service actually decreases during the equalization process, before increasing again and reaching the desired value. This may be caused by nonlinear inter-channel noise or power transfers phenomena across the channels when power changes on one OMS propagates to further OMSs [11, 12]. Commercial optical amplifiers can be set in either gain-lock or power-lock mode. While the power-lock could prevent undesired power propagation on downstream links, it also hinders fast rerouting after a failure; indeed, if services are rerouted on an OMS set to power-lock mode, the total OMS launch power will increase leading to a per-service power decrease and hence to suboptimal power allocation not only for the rerouted services, but also for the existing services. Operating amplifiers in gain-lock mode avoids this problem.

Hence, network-wide re-optimization and autonomous optical networking require the ability to search for a sequence of power adjustments whereby existing channels' SNRs do not degrade [13–15]. We propose to use an optical network digital twin as a sandbox to search for such a sequence. The digital twin implements real-time performance monitoring and SNR estimation/prediction.

In addition, an accurate SNR estimator requires accurate knowledge of the physical parameters. In real networks, the values of those parameters may be unknown, incorrect, or outdated, for instance when powers are changed during the re-optimization process. Online monitoring and updating of the physical parameters to close the monitoring–decide–act control loop is needed for accurate SNR prediction [13, 14].

This paper is an extended version of our conference paper at the European Conference on Optical Communication (ECOC) in 2024 [16]. By leveraging a digital twin, we are able to predict the SNR variation of all services in the network before carrying out any power adjustment operation. Using a specific search technique called multi-step lookahead, we find a sequence of power equalization steps that ensures monotonous SNR improvement for all services and avoid transient states whereby the SNR of some services is degraded during the network-wide power equalization process. Simultaneously changing the settings of multiple WSSes across several OMS sections, or even the two WSSes starting and terminating each OMS, is operationally infeasible. The paper introduces "WSS-parallel" adjustments to allow near-simultaneous operations, coordinated to minimize service disruption. This concept will be further elaborated in Section 2-B.3.

Compared with [16], in this paper we a) introduce and evaluate dynamic step-sizes instead of fixed power adjustment steps in the power equalization routine; b) evaluate the discrepancies between the current and target power profiles across various test configurations to assess optimization effectiveness. As in [16], this work is performed with a meshed optical network experimental testbed based on C-band commercial products.

This paper consists of five sections. In section 2, we introduce the principle of power equalization and present the proposed methodology. In section 3, we describe our experimental testbed and introduce four distinct experimental configurations to evaluate the proposed methodologies. In section 4, we present the impact of power propagation, show the power and SNR evolution of the four aforementioned scenarios, and analyze the digital twin time consumption. In section 5, we draw the conclusions and future directions.

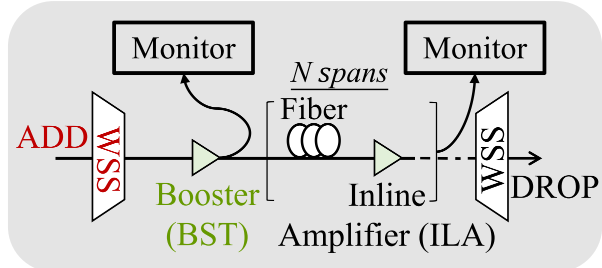

Fig. 2. Optical multiplexing section.

2. PRINCIPLE

A. Power Equalization

A.1. End-to-End SNR Optimization Method

A wavelength division multiplexing (WDM) based optical transport network consists of multiple OMSs. As shown in Fig. 2, each OMS has a pair of WSSes for routing/adding/dropping optical channels, N fiber spans and N+1 optical amplifiers (OAs), typically, erbium-doped fiber amplifier (EDFA). We refer to the first OA of each OMS as the booster, the other OAs after fiber spans are called inline amplifiers, and the last OA is also called pre-amplifier. We assume that the power spectra at the output of the booster and pre-amplifier, but not the online amplifiers, can be monitored. The launch power profile of the booster in an OMS can be tuned by adjusting the WSS attenuation profile, so that power equalization can be implemented to optimize the performance of services.

Before we discuss the end-to-end SNR of services, we first introduce the generalized SNR (GSNR). Unlike SNR, which accounts for end-to-end system effects including filtering penalties and transponder noise, GSNR excludes such factors and only includes amplified spontaneous emission (ASE) and non-linear (NL) noise contributions, such that GSNR is not only defined end-to-end, but also per-OMS. This differentiation is crucial for isolating the impact of power adjustments in optical networks.

Based on the Gaussian Noise (GN) model [6], the GSNR of a channel λ in an OMS is [17]:

$$GSNR_{OMS}(\lambda) = \frac{P_{ch}(\lambda)}{P_{ASE}(\lambda) + P_{NL}(\lambda)} = \frac{P_{ch}(\lambda)}{P_{ASE}(\lambda) + \eta(\lambda)P_{ch}^3(\lambda)} \quad \textbf{(1)}$$

where P_{ch} is the channel power, P_{ASE} is the ASE noise power, P_{NL} is the NL noise power, which is proportional to P_{ch}^3 with a ratio η.

GSNR varies with channel power, as shown in Fig. 3. By calculating the derivative of Eq. (1), GSNR maximization is achieved by balancing the ASE-to-NL noise ratio to 3dB [6], therefore, the optimal launch power of the channel in this OMS is:

$$P_{ch,OMS}^{opt}(\lambda) = \sqrt[3]{\frac{P_{ASE}(\lambda)}{2\eta}}. \quad \textbf{(2)}$$

Power optimization has garnered much attention recently, especially in the context of multi-band networks, but also for single-band networks [18–20]. We emphasize that the novel framework proposed here is orthogonal to the underlying power

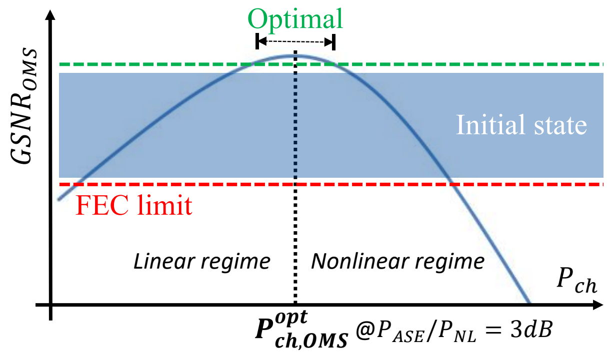

Fig. 3. GSNR and optimal launch power at $P_{ASE}/P_{NL} = 3dB$.

optimization —- should another equalization method be used, our framework applies identically.

For a service s carried by wavelength λ through route $OMS_1 - OMS_2 - \ldots - OMS_N$, the end-to-end (e2e) GSNR is [7]:

$$GSNR_{e2e}(s) = GNSR_{e2e}^{-1}(s) = \left(\sum_{n=1}^{N} GNSR_{OMS_n}(\lambda)\right)^{-1}, \quad (3)$$

where GNSR is the generalized noise-to-signal ratio, that is the inverse of GSNR.

Adding WSS distortion and transponder noises [21, 22], the e2e SNR can be written as:

$$SNR = NSR^{-1} = (f_{WSS,TRX}(GNSR) + NSR_{TRX})^{-1}, \quad (4)$$

where $f_{WSS,TRX}$ represents the filtering penalty from WSSes and noise scaling in transceiver (TRX), NSR_{TRX} represents the noise introduced by TRX, which can be calibrated in back-to-back (B2B) performance measurements.

SNRs estimated or measured throughout this paper are inherently end-to-end, capturing the cumulative impact of all the optical network elements on signal quality.

Booster launch power adjustment at an OMS yields power profile modification on the (downstream) OMSs by power propagation. Hence, the SNR of each service in the network may be impacted when adjusting the launch power spectrum on only one OMS. In the worst case, this possibly leads to disruption of existing services. We presented such a SNR degradation with large power adjustment step during the equalization [12].

A.2. Quantitative Metrics for Performance Evaluation

For such a network-wide power equalization, three metrics are evaluated.

First, we define the power error between the current channel power $P_{ch,n}(\lambda)$ and the target optimized power $P^{opt}_{ch,n}(\lambda)$ of the n^{th} OMS:

$$Err(P_{ch,n}(\lambda)) = P^{opt}_{ch,n}(\lambda) - P_{ch,n}(\lambda). \quad (5)$$

Second, we define the network-wide SNR margin as:

$$SNR_{margin} = \min_{s}(SNR(s) - SNR_{FEC}(s)), \quad (6)$$

where $SNR(s), s = 1, ..., N_{svc}$ is the SNR of services s, and $SNR_{FEC}(s)$ is the SNR at the limit of forward error correction (FEC) for service s. The SNR margin represents the performance of bit-error-rate (BER) [21, 23]. If $SNR(s) < SNR_{FEC}(s)$, then uncorrected blocks will appear. Therefore, the SNR margin should always be positive during any optical network operation. The higher SNR margin, the lower pre-FEC BER, which can then be leveraged to carry additional traffic / increase the network capacity.

The third metric is the total network (Shannon) capacity C:

$$C = 2\sum_{s=1}^{N_{svc}} log_2(1 + SNR(s)). \quad (7)$$

The average absolute power error $Avg(|Err(P_{ch,n})|)$ shows how far the current state is from the optimized (target) state. We use this metric as the most important convergence criterion for the optimization algorithm presented later. The SNR margin quantifies the performance of the worst service in the network, and should remain (as much) positive (as possible). The capacity C quantifies the global performance of all services in the network.

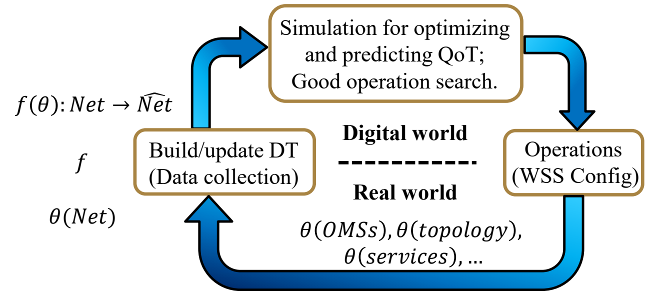

Fig. 4. Digital twin enabled power equalization.

B. Digital Twin Enabled Power Equalization

Beyond balancing the ASE/NL ratio, other power equalization methods are possible. The methodology we propose here is generic and independent of the specific power equalization strategy used in the network, see Fig. 4: We build the digital twin and periodically update it based on physical parameters monitored in the network.

$$f(\theta) : Net \rightarrow \widehat{Net}, \quad (8)$$

where θ represents the physical parameters from the real world, including power spectra, gain/tilt of OAs, fiber parameters in the OMSs, topology and services information of network, etc. Later, we use hat to represent the processes in the digital world.

Then, we find the order of the operations along with the power variation step-size, and assess the impact of those changes on the QoT of all services using a QoT estimator, before implementing the operations in the network to prevent potential QoT degradations.

B.1. Multi-Step Lookahead Prediction with Fixed Step-Size

Multi-step lookahead in chess is the ability to anticipate and evaluate potential move sequences several turns ahead, considering both the player's and the opponent's responses. This strategic foresight enables players to plan, exploit opportunities, and avoid risks effectively.

In the power equalization problem, the multi-step lookahead method can avoid local optimum step-searching thereby reducing the total time consumption.

Algorithm 1 presents the workflow of multi-step lookahead prediction and configuration of an optical network with fixed step-size.

First, data collection is needed for building/updating digital twin (line 2). However, it is not necessary to update the digital

Algorithm 1. Multi-step lookahead prediction for power equalization

```
1:  while NOT optimized for all $\widehat{OMS}$ (Condition-1/2/3) do
2:      Update digital twin
3:      Find the optimal launch power per $\widehat{OMS}$ by Eq.(2)
4:      for $k = 1, ..., K_{update}$ do
5:          for $m = 1, ..., K_m$ do
6:              for $n = 1, ..., N_{OMS}$ do
7:                  for $\lambda = 1, ..., N_{CH(n)}$ do
8:                      Adjust booster $\widehat{P_n}(\lambda)$ by Eq.(9)
9:                  Power propagation in digital twin
10:                 $\widehat{SNR}$ prediction in digital twin
11:         Find the $K_m$-step order of operations which yields the highest $\widehat{SNR}_{margin}$ by Eq.(11)
12:     Configure the WSS
```

twin after each step. Instead, we update our digital twin every K_{update}-steps (line 4).

Second, assuming there are N_{OMS} non-optimized $\widehat{OMS}$, the optimal launch power profiles of these $\widehat{OMS}$s are found by digital twin based on Eq. (2) $\widehat{P_{ch,n}^{opt}}(\lambda)$ (line 3) .

Third, for K_m-step lookahead (lines 5-11), the digital twin emulates the power adjustment impact on different $\widehat{OMS}$s (line 6). The fixed step adjustment (line 8) of launch power $\widehat{P_{ch,n}}(\lambda)$ of each channel of n^{th} $\widehat{OMS}$ given by:

$$\Delta\widehat{P_n}(\lambda) = \begin{cases} \widehat{P_{ch,n}^{opt}}(\lambda) - \widehat{P_{ch,n}}(\lambda), & if |Err(\widehat{P_{ch,n}}(\lambda))| < \delta \\ \delta \cdot sign(Err(\widehat{P_{ch,n}}(\lambda))), & otherwise \end{cases} \tag{9}$$

where δ is a fixed, predefined power adjustment step-size. Then, the digital twin predicts the $\widehat{SNR}$ (line 10) after the power propagation (line 9).

For K_m-step lookahead within a N_{OMS}-OMS network, there are up to $N_{OMS}^{K_m}$ possible sequences (this is an upper bound because if an operations decrease the margin at some step, then the algorithm will not pursue the branch):

$$seq\{k_i\} = (\widehat{OMS}_{k_1}, \ldots, \widehat{OMS}_{k_i}, \ldots, \widehat{OMS}_{k_{K_m}}), \tag{10}$$

where $i \in \{1, 2, ..., K_m\}$, and $k_i \in \{1, 2, ..., N_{OMS}\}$.

For each sequence, line 10 yields an $\widehat{SNR}$ variation after power propagation $\Delta\widehat{SNR}_{seq\{k_i\}}$. Therefore, the digital twin picks up the order of operations (on which $\widehat{OMS}$) yields the highest $\widehat{SNR}_{margin}$ (line 11):

$$\begin{cases} \underset{seq\{k_i\}}{max}\ \Delta\widehat{SNR}_{seq\{k_i\}}, \\ \Delta\widehat{SNR}_{k_i} > \epsilon_{SNR}, \end{cases} \tag{11}$$

where ϵ_{SNR} is the tolerance of $\widehat{SNR}$ drop during the multi-step operations. To avoid oscillations/local optima, the multi-step lookahead algorithm allows small $\widehat{SNR}$ drops at intermediate steps k_i in case this yields a higher $\widehat{SNR}$ after all K_m steps.

Then, the digital twin will configure the WSS (line 13) following the order from line 11, until all $\widehat{OMS}$s are optimized (line 1).

Algorithm 2. Multi-step lookahead prediction for power equalization with dynamic step-size

```
1:  while NOT optimized for all $\widehat{OMS}$ (Condition-1/2/3) do
2:      Update digital twin
3:      Find the optimal launch power per $\widehat{OMS}$ by Eq.(2)
4:      for $k = 1, ..., K_{update}$ do
5:          for $m = 1, ..., K_m$ do
6:              for $n = 1, ..., N_{OMS}$ do
7:                  for $\delta = \delta_{max}, ..., \delta_{min}$ do
8:                      for $\lambda = 1, ..., N_{CH(n)}$ do
9:                          Adjust booster $\widehat{P_n}(\lambda)$ by Eq.(9), Eq.(15)
10:                     Power propagation in digital twin
11:                     $\widehat{SNR}$ prediction in digital twin
12:         Find the $K_m$-step order of operations which yields the highest $\widehat{SNR}_{margin}$ or maximizes power error reduction, in a safe way (Eq. 16)
13:     Configure the WSS
```

The convergence of the algorithm, or the stop-while condition, could be defined by using the metrics in Eq. (5-7):

Condition-1: average power error tolerance ε_{Perr}.

$$Avg(|Err(\widehat{P_{ch,n}})|) \leq \varepsilon_{Perr}. \tag{12}$$

Condition-2: max SNR margin error from ideal value ε_{margin}. Defining $max_{th}(\widehat{SNR}_{margin})$ the max theoretical SNR margin achievable in digital twin.

$$|\widehat{SNR}_{margin} - max_{th}(\widehat{SNR}_{margin})| \leq \varepsilon_{margin}. \tag{13}$$

Condition-3: capacity (overall SNR) error from ideal value ε_C. Defining $max_{th}(\widehat{C})$ the max theoretical capacity achievable in digital twin.

$$|\widehat{C} - max_{th}(\widehat{C})| \leq \varepsilon_C. \tag{14}$$

These conditions can be used alone or in combination.

B.2. Dynamic Step-Size for Power Adjustment

As we presented in [16], when the optical network was close to the optimized state, the measured SNR_{margin} was higher and increased slowly or even oscillated. To speed up convergence, a larger step-size could be considered and SNR_{margin} might no longer be the best metric when operations are selected in the digital twin. Then, we propose the Algorithm 2.

There are two differences compared with the Alg. 1.

1) Given a max step-size δ_{max}, a min step-size δ_{min} and interval $\Delta\delta$, the step-size is dynamically adjusted (line 7 in Algorithm 2) within the range:

$$\delta = \delta_{min}, \delta_{min} + \Delta\delta, ..., \delta_{max} - \Delta\delta, \delta_{max}. \tag{15}$$

The loop starting line 7 predicts the $\widehat{SNR}$ after changing the launch power by a step-size in the above range. A larger step-size yields more power fluctuation and has higher probability to decrease the $\widehat{SNR}_{margin}$. Hence, the algorithm dynamically adjusts the step-size, starting from a large value, to find the max step-size δ ensuring safety yet minimizing the number of operations. For each step in line 9, we apply the above δ into Eq. (9).

2) The difference between line 11 in Alg. 1 and line 12 in Alg. 2 lies in the action search order; once the $\widehat{SNR}_{margin}$ is

higher enough, digital twin will try to search the step orders which improves the $\widehat{SNR}_{margin}$ and reduces more power error $\Delta Avg(|Err(\widehat{P_{ch,n}})|)_{seq\{k_i\}}$ between current state profile and target state, instead of focusing on $\widehat{SNR}_{margin}$ only.

$$\begin{cases} \Delta\widehat{SNR}_{seq\{k_i\}} > 0, \\ \max\limits_{seq\{k_i\}} \Delta Avg(|Err(\widehat{P_{ch,n}})|)_{seq\{k_i\}}. \end{cases} \tag{16}$$

B.3. Parallel Configuration

Without prediction of $\widehat{SNR}$, the parallel configuration is risky for the optical network since the commands cannot be guaranteed to arrive at all network elements synchronously; intermediate states may interrupt services.

Instead, based on the multi-step lookahead, we can send the commands for K_m operations at the same time even if the WSS adjustments will not be strictly simultaneous, since prior emulation within the digital twin ensures no $\widehat{SNR}$ degradation for any service, whatever the order in which the commands are actually received by the physical layer from the digital twin, and executed within the physical layer.

C. Time Consumption of Digital Twin Enabled Auto-Adjustment of Power

In the control loop shown in Fig. 1. We can write the total commissioning time T_{tot} as:

$$T_{tot} = T_{update} + T_{sim} + T_{op}, \tag{17}$$

where T_{update} is the total time consumption for updating the digital twin, T_{sim} is the total simulation time in the QoT tool including optimization and $\widehat{SNR}$ prediction, T_{op} is total operation time for WSS setting. Specifically:

$$T_{update} = (\lceil N_{op}/K_{update} \rceil + 1) \cdot t_{update}, \tag{18}$$

where N_{op} is the total number of power adjustment steps, $\lceil\rceil$ is the ceiling function, and the digital twin is updated (through monitoring) every K_{update} power adjustment steps. Including the initialization, there are $\lceil N_{op}/K_{update} \rceil + 1$ updates. t_{update} is the time to collect data from the physical layer to update the entire digital twin.

$$T_{sim} = (N_{op} + 1) \cdot t_{sim}, \tag{19}$$

where t_{sim} is the time to run the $\widehat{SNR}$ prediction tool and run the proposed algorithm in the digital twin; there are $N_{op} + 1$ simulations needed for each operation and the initialization.

$$T_{op} = N_{op} \cdot t_{WSS}, \tag{20}$$

t_{WSS} is the time needed to configure the attenuation profile of WSS, thereby adjusting the launch power.

The time complexity of Alg. 1 to generate the next step is $\mathcal{O}(\frac{1}{K_m} N_{OMS}^{K_m})$. Hence, the trade-off between K_m and computation power also needs to be considered during commissioning. For a network with N_{OMS} where OMS_n has $N_{span(n)}$ spans, the upper bound for simulation time t_{sim} in Eq. (19) is:

$$t_{sim} \le \frac{1}{K_m} (\sum_{n}^{N_{OMS}} N_{span}(n))^{K_m} \cdot t_{sim,span}, \tag{21}$$

where $t_{sim,span}$ is average simulation time per span. If any of the K_m steps results in a significant degradation of the $\widehat{SNR}$, no further simulation of this step will be performed, hence Eq. (21) is indeed an upper bound.

Without considering any parallel data collection for updating the digital twin, the update time t_{update} in Eq. (18) can be written as:

$$t_{update} = \sum_{n}^{N_{OMS}} t_{update}(n) = \sum_{n}^{N_{OMS}} 2t_{mon} + (N_{span}(n) + 1)t_{OA}, \tag{22}$$

where t_{mon} is the time to get a power profile by the monitor, and t_{OA} is the time to collect data (gain, total in/output power) from an OA. The parameters refinement technique from [24] can be used to estimate the OA gain profile and lumped losses so that power monitoring is only needed for the first and last optical amplifiers of each OMS.

If monitoring data for all OMSs is collected in parallel, Eq. (22) becomes:

$$t_{update} = max_n(t_{update}(n) + t_{delay}(n)), \tag{23}$$

where t_{delay} is the communication time between the controller and equipment on OMS_n.

Normally, $t_{update}(n)$ is in the order of seconds while $t_{sim,span}$ is in the order of ms, then $t_{update} \gg t_{sim}$ for $K_m = 1$ and any N_{OMS}. However, it may not be true in some scenarios if $K_m \ge 2$ with a large N_{OMS}.

For instance, consider a homogeneous network in which each OMS has the same number of spans N_{span}. Then, for an upper bound on t_{sim}:

$$t_{sim} = N_{OMS}^{K_m - 1} N_{span}^{K_m} \cdot t_{sim,span}, \tag{24}$$

$$t_{update} = N_{OMS}(2t_{mon} + (N_{span} + 1)t_{OA}), \tag{25}$$

The ratio t_{sim}/t_{update} is then:

$$\frac{t_{sim}}{t_{update}} = \frac{1}{K_m} N_{OMS}^{K_m - 1} N_{span}^{K_m} \cdot r_t, \tag{26}$$

where $r_t = \frac{t_{sim,span}}{2t_{mon} + (N_{span}+1)t_{OA}}$. Depending on the data collection time and computing resource for the digital twin, ratio r_t is typically smaller than 1/100. The time consumption could be very large when the network scales or we look a larger K_m ahead. When $K_m = 2$, the factor $\frac{1}{K_m} N_{OMS}^{K_m-1} N_{span}^{K_m} = \frac{1}{2} N_{OMS} N_{span}^2$ is still linear with N_{OMS}. However, if $K_m > 2$, then the factor $\frac{1}{K_m} N_{OMS}^{K_m-1} N_{span}^{K_m}$ is no longer linear (quadratic, ...) with N_{OMS}.

In this paper, we only consider the scenarios with $K_m \le 2$, our proposed methods focus on reducing the number of operations N_{op}, thereby decreasing the total time consumption T_{tot}.

3. EXPERIMENTAL SETUP

A. Network Topology

The commercial products-based testbed has a meshed network topology, as shown in Fig. 5.

The OMSs are heterogeneous, containing heterogeneous fiber spans and different types of amplifiers. The fiber types include G.652.D standard single model fiber (SMF), G.654.E pure-silica-core fiber (PSCF), G.655.D large effective area fiber (LEAF) and G.655.D true-wave fiber (TW). The system operates in the C-band, and EDFA is the only type of optical amplifier used in the network, the gain and tilt of EDFAs were pre-configured and not adjusted during the experiments. The EDFAs shown in

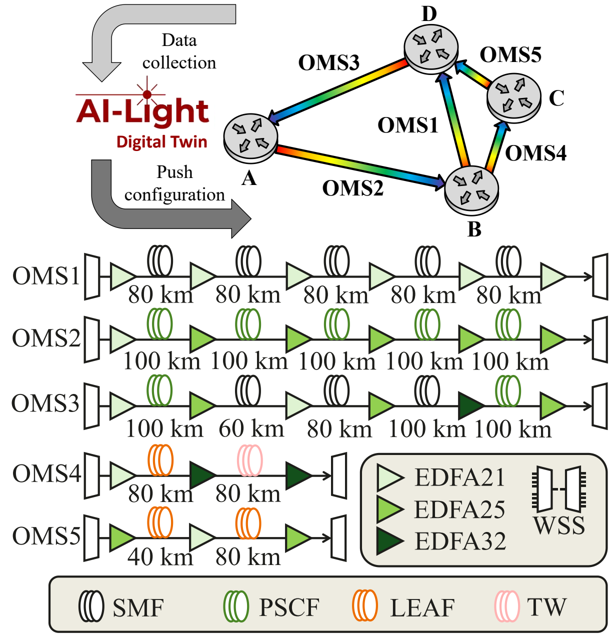

Fig. 5. Experimental setup.

Fig. 5 have various tunable gain range, EDFA21 has a range of 16-21dB, EDFA25 has a range of 19-25dB, EDFA32 has a range of 23-32dB. The WSS grid is set to 100 GHz channel spacing within the 6 THz C-band.

B. Service Loading and Monitoring

We emulated 95 services using ASE loading in the network and emulated set-and-forget loading (i.e., the power of a service may drift as further services are established,) such that channels are not well equalized.

We emulated launch power in this experiment following [10] as a Gaussian distribution with 0dB mean and 1dB standard deviation.

A real-time 400 Gb/s (PDM-PCS16QAM) transponder is used to replace the ASE loading during the SNR measurements. For experimental assessment of the SNR margin of the network, we use this transponder to measure the pre-FEC BER of the 5 worst services as reported by the digital twin and convert into SNR. All services have the same FEC limit SNR_{FEC}, therefore, the network-wide SNR margin simplifies to $min_s SNR(s) - SNR_{FEC}$ (from Eq. 6).

The testbed is automated with our software-defined networking (SDN) framework named AI-Light [25]. The SDN controller collects the data from the physical layer and implements/updates the digital twin to perform the proposed algorithm.

The digital twin needs periodic updates due to the OA gain profile variation caused by the launch power profile variation. We do not collect the gain profiles directly since most operators deploy per-channel power monitoring only at the output of booster and pre-amplifier. We apply the parameters refinement technique to refine the OA gain profile (as well as connector losses, which also cannot be directly measured) as in [24].

During each update cycle, the DT collects real-time data from the physical network, including power spectra at the output of boosters and pre-amplifiers, total input/output power of all OAs, as well as the configured values for gain and tilt of all OAs. The power spectra is monitored by optical spectrum analyzer in the testbed.

C. Algorithm Configurations and Example

In this work, we carry out the experiments for 4 different cases:

Case-1: 1-step lookahead with fixed 1dB step-size ($K_m = 1, \delta = 1dB$);

Case-2: 2-step lookahead with fixed 1dB step-size ($K_m = 2, \delta = 1dB$);

Case-3: 1-step lookahead with dynamic step-size ($K_m = 1, \delta_{min} = 1dB, \delta_{max} = 3dB, \Delta\delta = 0.5dB$); to compare with Case-1, we do not use 2-step lookahead for this case and keep the same K_m as in Case-1;

Case-4: 2-step lookahead with fixed 1dB step-size and parallel setting ($K_m = 2, \delta = 1dB$).

($K_{update} = 2$ and $\epsilon_{SNR} = -0.5dB$ for all the cases.)

Sample algorithms execution:

Initialization and data collection: The algorithm begins by initializing the digital twin with the current state of the physical network. The digital twin collects real-time data, including power spectra at the output of boosters and pre-amplifiers, configured gain/tilt of OAs, total in/output power of OAs.

Iterations:

- Digital twin update: The digital twin is updated with new real-time data to reflect the changes made in the previous iteration.
- Optimal launch power calculation: The digital twin computes the optimal launch power profile for each $\widehat{OMS}$ based on the updated network state.
- Power adjustment simulation: The digital twin simulates the impact of adjusting the power settings using either a fixed step-size or dynamic step-size. The digital twin predicts the resulting $\widehat{SNR}$ for each service after power propagation.
- Operation selection: The algorithm selects the sequence of operations that yields the highest $\widehat{SNR}_{margin}$ without degrading any service's $\widehat{SNR}$. For instance, for a 5-OMS network, if $K_m = 2$ (prediction are 2 changes ahead), possible operation sequences are ($\widehat{OMS}_i$, $\widehat{OMS}_j$) i.e. optimize $\widehat{OMS}_i$ then $\widehat{OMS}_j$, which improves the $\widehat{SNR}$ by $\Delta\widehat{SNR}_{i,j}$, and the sequence $(\widehat{OMS}_k, \widehat{OMS}_l) = \underset{i,j \in \{1,2,3,4,5\}}{argmax} \Delta\widehat{SNR}_{i,j}$ is selected.
- WSS configuration: The digital twin controller configures the WSSes in the physical network according to the selected sequence of operations.

Convergence: The algorithm repeats the above steps until the convergence criteria are met. The convergence criterion is defined as an average power error of less than 0.5dB such that the algorithm converges to a state where $\widehat{SNR}_{margin}$ is maximized, and the power settings are balanced across all $\widehat{OMS}$s. We cap the number of iterations in case convergence is not achieved.

4. RESULTS

A. Power Propagation and SNR Degradation

We already presented that open-loop and sequential setting with one-shot ($\Delta P_n(\lambda) = P^{opt}_{ch,n}(\lambda) - P_{ch,n}(\lambda)$) could significantly degrade some services' SNR in point-to-point [11] and ring [12] networks. In this work, we also observe such an SNR degradation in the meshed network due to the power propagation in Fig. 6.

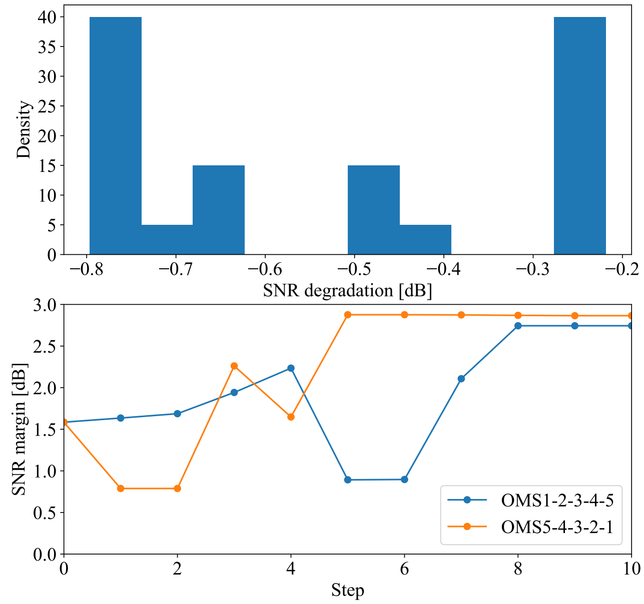

Fig. 6. SNR degradation with open-loop. Top: Simulation results of SNR degradation value with 120 different orders. Bottom: SNR margin variation with different operation orders.

For a 5-OMS network, there are $5! = 120$ possible one-shot OMS adjustment sequences. From the simulation results shown in Fig. 6(top), we observe that regardless of the adjustment sequence, the SNR deteriorates compared to the initial value during the process. Fig. 6(bottom) illustrates two of these cases. In addition to the SNR degradation, it is noteworthy that nearly 10 one-shot adjustments are required to achieve the target, optimized state in the 5-OMS network. This is primarily due to power propagation: although the power of one OMS is equalized in a single step, adjustments to the power of other OMSs cause power propagation, leading to deviations from the optimized state in previously equalized OMSs, which then need to be re-equalized.

B. Power Error

In the subsequent experimental results, we demonstrate that even with a smaller fixed step-size, it is possible to complete global power equalization efficiently.

We use Condition 1 (Eq. (12)) with $\varepsilon_{Perr} = 0.5dB$ as the convergence criterion. Fig. 7 shows the variation of average power error with respect to the number of operational steps for the four cases defined above. For Case-1, it is evident that local rather than global optimization is achieved: OMS5 struggles to converge, resulting in a total of 31 steps. In Case-2, with multi-step prediction, the process escapes the local optimization trap and satisfies the convergence criterion for average power error in 18 steps. Compared to Case-1, Case-3 employs dynamic step-size adjustment and dynamic metric selection, achieving power equalization in just 14 steps. Although Case-4 still uses a small fixed step-size adjustment, parallel adjustment allows for faster overall power equalization, converging in only 13 steps.

From Fig. 7, we can summarize the distinctive characteristics of average power error reduction across the four cases: Case-1 exhibits symptoms of local optimization; Case-2 overcomes this limitation; Case-3 shows a significantly steeper error reduction slope; and Case-4 motivates parallel equalization.

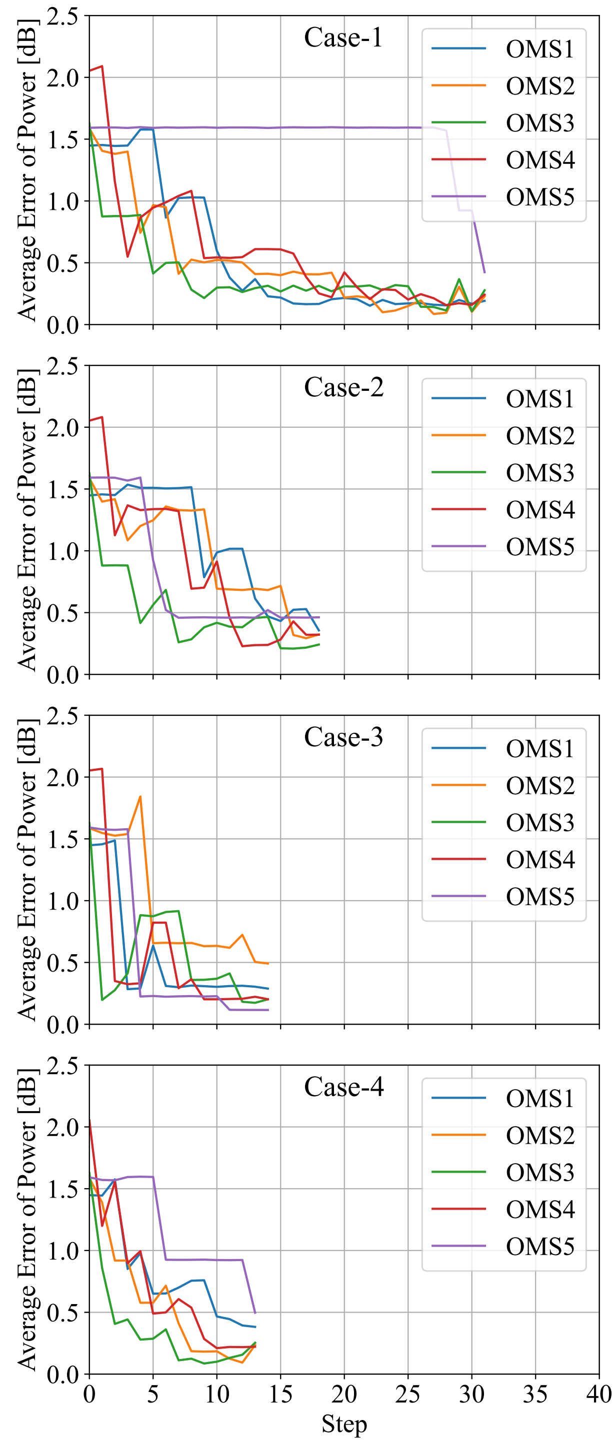

Fig. 7. Average error of between current channel power and target channel power with steps. Case-1: 1-step lookahead with 1dB step-size; Case-2: 2-step lookahead with 1dB step-size; Case-3: 1-step lookahead with dynamic step-size; Case-4: 2-step lookahead with 1dB step-size and parallel setting.

C. SNR Margin and Overall Evolution

As shown in Fig. 8, SNR_{margin} is improved by ∼1.5dB through power optimization. The plots include digital twin-*predicted* values (using monitoring data from before an operation; empty circle), the measured value after an operation (plain circle), and also the digital twin-*estimated* value (using monitoring data from

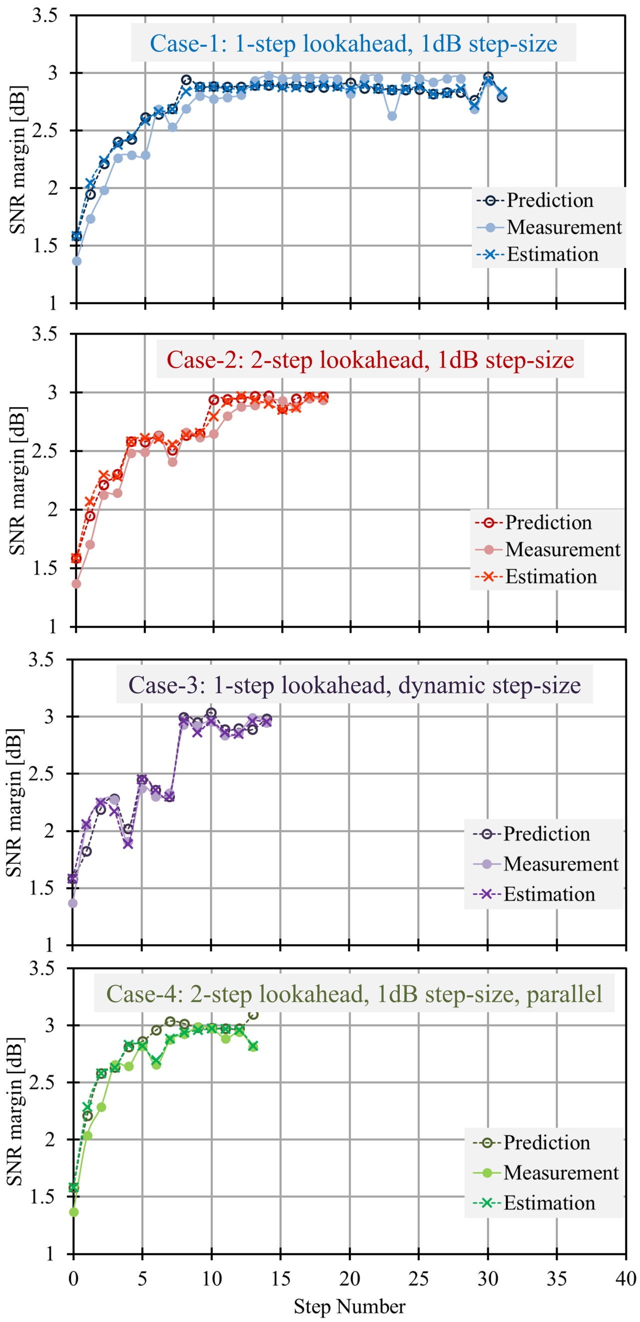

Fig. 8. SNR margin with different scenarios. Case-1: 1-step lookahead with 1dB step-size; Case-2: 2-step lookahead with 1dB step-size; Case-3: 1-step lookahead with dynamic step-size; Case-4: 2-step lookahead with 1dB step-size and parallel setting.

after operation; cross). It shows good alignment between results from the digital twin (both a-priori prediction and a-posteriori estimate) and measurements.

The SNR_{margin} converges in only 10 steps for all strategies (Fig. 8), however, total capacity converges more slowly (Fig. 9), which consistent with the average power error evolution (Fig. 7).

D. Time Consumption Analysis

Then, we compute the total commissioning time by applying Eq. (17)-(22). Data collection is not parallel in our testbed. The

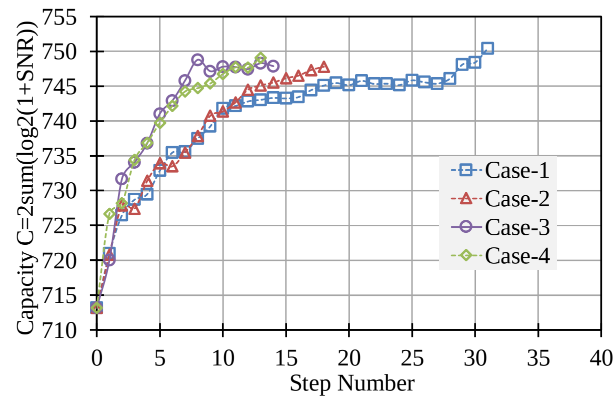

Fig. 9. System capacity, or overall SNR. Case-1: 1-step lookahead with 1dB step-size; Case-2: 2-step lookahead with 1dB step-size; Case-3: 1-step lookahead with dynamic step-size; Case-4: 2-step lookahead with 1dB step-size and parallel setting.

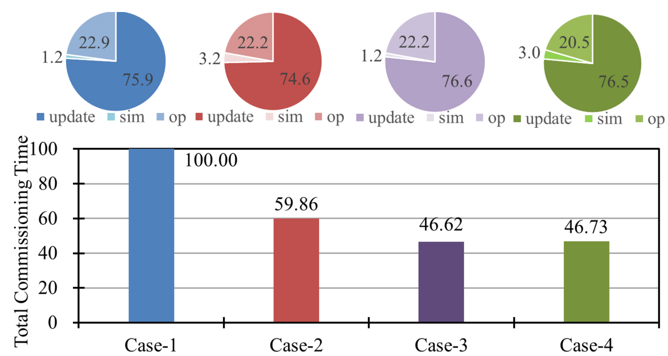

Fig. 10. Time consumption analysis. Case-1: 1-step lookahead with 1dB step-size; Case-2: 2-step lookahead with 1dB step-size; Case-3: 1-step lookahead with dynamic step-size; Case-4: 2-step lookahead with 1dB step-size and parallel setting.

results are shown in Fig. 10, normalized to Case-1 (as baseline) commissioning time (set to 100 for convenience).

Compared with Case-1, the proposed algorithm can save 40%(Case-2)/53%(Case-3)/53%(Case-4) of T_{tot}. The pie chart reveals that the major cost of T_{tot} is spent on updating the digital twin, indicating that increasing K_{update} to reduce update times could further save time.

The quantitative comparison is shown in Tab. 1 and we summarize the advantages and disadvantages of different cases in Tab. 2.

5. CONCLUSIONS AND FUTURE PERSPECTIVES

In this paper, we demonstrated the significant potential of digital twins to enable automated and optimized power equalization in optical networks. By integrating multi-step lookahead prediction and dynamic step-size adjustments, our proposed methodology ensures consistent improvements in SNR margins and efficient convergence to optimal power states without service disruptions. Experimental validation on a meshed optical network testbed confirmed substantial reductions in power errors, enhanced SNR performance, and a marked decrease in commissioning time, highlighting the practical feasibility of our approach. These findings emphasize the transformative

Table 1. Quantitative Metrics Comparison

Case	1	2	3	4
K_m	1	2	1	2
Step-size [dB]	1	1	dynamic	1
Parallel	No	No	No	Yes
Number of steps to convergence	31	18	14	13
Total commissioning time [normalized]	100	60	47	47
Final SNR margin improvement [dB]	1.6	1.5	1.6	1.5
Final capacity improvement [%]	5.2	4.9	5.1	4.9

Table 2. Qualitative Evaluation

Case	Conclusion
1	(baseline)
2	Avoids local optima and oscillations.
3	Faster (with larger steps) but more prone to temporarily low SNR margin.
4	Even faster during operation (parallel operation) but need to check all possible WSS change orderings in the digital twin.

role of digital twins in advancing autonomous optical network management by enabling precise, non-disruptive, and efficient network-wide optimizations.

While this work focused on reducing the total number of WSS attenuation adjustment operations and analyzing the time consumption across different components of the workflow, future research could extend these methodologies to include gain and tilt adjustments for OAs. Additionally, optimizing the time consumption of individual components within the workflow could further enhance real-time applicability, broadening the scope of digital twin applications in optical network automation.

REFERENCES

1. D. Wang, Y. Song, Y. Zhang, X. Jiang, J. Dong, F. N. Khan, T. Sasai, S. Huang, A. P. T. Lau, M. Tornatore, and M. Zhang, "Digital Twin of Optical Networks: A Review of Recent Advances and Future Trends," J. Light. Technol. **42**, 4233–4259 (2024).
2. Q. Zhuge, X. Liu, Y. Zhang, M. Cai, Y. Liu, Q. Qiu, X. Zhong, J. Wu, R. Gao, L. Yi, and W. Hu, "Building a digital twin for intelligent optical networks [Invited Tutorial]," J. Opt. Commun. Netw. **15**, C242–C262 (2023).
3. R. Vilalta, L. Gifre, R. Casellas, R. Muñoz, R. Martínez, A. Mozo, A. Pastor, D. López, and J. P. Fernández-Palacios, "Applying Digital Twins to Optical Networks with Cloud-Native SDN Controllers," IEEE Commun. Mag. **61**, 128–134 (2023).
4. M. S. Faruk and S. J. Savory, "Measurement Informed Models and Digital Twins for Optical Fiber Communication Systems," J. Light. Technol. **42**, 1016–1030 (2024).
5. Y. He, Z. Zhai, L. Dou, L. Wang, Y. Yan, C. Xie, C. Lu, and A. P. T. Lau, "Improved QoT estimations through refined signal power measurements and data-driven parameter optimizations in a disaggregated and partially loaded live production network," J. Opt. Commun. Netw. **15**, 638–648 (2023).
6. P. Poggiolini, G. Bosco, A. Carena, V. Curri, Y. Jiang, and F. Forghieri, "The GN-Model of Fiber Non-Linear Propagation and its Applications," J. Light. Technol. **32**, 694–721 (2014).
7. A. Ferrari, "Physical Layer Aware Open Optical Networking," Ph.D. thesis, Politecnico di Torino, Turin, Italy (2021).
8. Y. Zhang, X. Pang, Y. Song, Y. Wang, Y. Zhou, H. Zhu, L. Zhang, Y. Fan, Z. Guo, S. Huang, M. Zhang, and D. Wang, "Optical Power Control for GSNR Optimization Based on C+L-Band Digital Twin Systems," J. Light. Technol. **42**, 95–105 (2024).
9. X. Liu, Y. Zhang, M. Cai, Y. Liu, L. Yi, W. Hu, and Q. Zhuge, "SMOF: Simultaneous Modeling and Optimization Framework for Raman Amplifiers in C+L-Band Optical Networks," J. Light. Technol. **42**, 3174–3183 (2024).
10. X. Yang, A. Ferrari, D. L. Gac, G. Charlet, M. Tornatore, and Y. Pointurier, "Experimental impact of power re-optimization in a mesh network," J. Opt. Commun. Netw. **15**, C20–C28 (2023).
11. C. Sun, X. Yang, G. Charlet, P. A. Stavrou, and Y. Pointurier, "Digital Twin-Enabled Service Optimization Sequence of Actions for Power Equalization," in *2023 Asia Communications and Photonics Conference/2023 International Photonics and Optoelectronics Meetings (ACP/POEM),* (2023).
12. C. Sun, X. Yang, G. Charlet, P. A. Stavrou, and Y. Pointurier, "Digital Twin-Enabled Optical Network Automation: Power Re-Optimization," in *Optical Fiber Communication Conference (OFC) 2024,* (Optica Publishing Group, 2024), p. W4I.5.
13. K. Christodoulopoulos, C. Delezoide, N. Sambo, A. Kretsis, I. Sartzetakis, A. Sgambelluri, N. Argyris, G. Kanakis, P. Giardina, G. Bernini, D. Roccato, A. Percelsi, R. Morro, H. Avramopoulos, P. Castoldi, P. Layec, and S. Bigo, "Toward efficient, reliable, and autonomous optical networks: the ORCHESTRA solution [Invited]," J. Opt. Commun. Netw. **11**, C10–C24 (2019).
14. A. Mahajan, K. K. Christodoulopoulos, R. Martínez, R. Muñoz, and S. Spadaro, "Quality of transmission estimator retraining for dynamic optimization in optical networks," J. Opt. Commun. Netw. **13**, B45–B59 (2021).
15. H. Zhang, F. Gao, J. Cheng, L. Dou, S. Chen, B. Yan, Z. Sun, L. Wang, and C. Xie, "Demonstration of a Disaggregated ROADM Network with Automatic Channel Provisioning and Link Power Adjustment," in *2021 European Conference on Optical Communication (ECOC),* (2021).
16. C. Sun, X. Yang, G. Charlet, P. A. Stavrou, and Y. Pointurier, "Digital Twin Enabled Automatic Power Adjustment with Multi-Step Lookahead Prediction," in *50th European Conference on Optical Communication (ECOC),* (2024), p. M2E.1.
17. D. Semrau, R. I. Killey, and P. Bayvel, "A closed-form approximation of the gaussian noise model in the presence of inter-channel stimulated raman scattering," J. Light. Technol. **37**, 1924–1936 (2019).
18. H. Buglia, R. I. Killey, and P. Bayvel, "Ultra-wideband modeling of optical fibre nonlinearity in hybrid-amplified links," J. Light. Technol. **42**, 8664–8677 (2024).
19. K. Nikolaou, D. Uzunidis, F. Arpanaei, J. M. Rivas-Moscoso, D. Larrabeiti, and I. Tomkos, "Maximizing the transport capacity of optical multi-band wdm systems through power optimization," in *2024 International Conference on Optical Network Design and Modeling (ONDM),* (2024).
20. G. Borraccini, S. Straullu, A. D'Amico, F. Aquilino, S. Piciaccia, A. Tanzi, G. Galimberti, and V. Curri, "Local and global optimization methods for optical line control based on quality of transmission," J. Opt. Commun. Netw. **16**, B60–B70 (2024).
21. Y. Pointurier, "Design of low-margin optical networks," J. Opt. Commun. Netw. **9**, A9–A17 (2017).
22. I. F. de Jauregui Ruiz, A. Ghazisaeidi, T. Zami, S. Louis, and B. Lavigne, "An accurate model for system performance analysis of optical fibre networks with in-line filtering," in *45th European Conference on Optical Communication (ECOC),* (2019).
23. S. J. Savory, R. J. Vincent, and D. J. Ives, "Design considerations for

low-margin elastic optical networks in the nonlinear regime [invited]," J. Opt. Commun. Netw. **11**, C76–C85 (2019).

24. N. Morette, H. Hafermann, Y. Frignac, and Y. Pointurier, "Machine learning enhancement of a digital twin for wavelength division multiplexing network performance prediction leveraging quality of transmission parameter refinement," J. Opt. Commun. Netw. **15**, 333–343 (2023).
25. A. Ferrari, V. V. Garbhapu, D. L. Gac, I. F. de Jauregui Ruiz, G. Charlet, and Y. Pointurier, "Demonstration of AI-Light: an Automation Framework to Optimize the Channel Powers Leveraging a Digital Twin," in *Optical Fiber Communication Conference (OFC) 2022,* (Optica Publishing Group, 2022), p. M3Z.14.